*Journal of Fusion Energy, Vol. 9, No. 2, 1990*

# Measurement and Analysis of Neutron and Gamma-Ray Emission Rates, Other Fusion Products, and Power in Electrochemical Cells Having Pd Cathodes

**David Albagli,[1] Ron Ballinger,[3,4] Vince Cammarata,[1] X. Chen,[2] Richard M. Crooks,[1] Catherine Fiore,[2] Marcel P. J. Gaudreau,[2] I. Hwang,[3,4] C. K. Li,[2] Paul Linsay,[2] Stanley C. Luckhardt,[2] Ronald R. Parker,[2,5] Richard D. Petrasso,[2] Martin O. Schloh, [1] Kevin W. Wenzel,[2] and Mark S. Wrighton[1,5]**

Results of experiments intended to reproduce cold fusion phenomena originally reported by Fleischmann, Pons, and Hawkins are presented. These experiments were performed on a pair of matched electrochemical cells containing 0.1 × 9 cm Pd rods that were operated for 10 days. The cells were analyzed by the following means: (1) constant temperature calorimetry, (2) neutron counting and γ-ray spectroscopy, (3) mass spectral analysis of $^4$He in effluent gases, and $^4$He and $^3$He within the Pd metal, (4) tritium analysis of the electrolyte solution, and (5) x-ray photoelectron spectroscopy of the Pd cathode surface. Within estimated levels of accuracy, no excess power output or any other evidence of fusion products was detected.

**KEY WORDS:** Fusion; cold fusion; palladium; excess heating.

## 1. INTRODUCTION

There have been three recent reports of nuclear fusion processes occurring at room temperature inside metal lattices.[1-3] Two of these[2,3] report only very low levels of neutron emission, and although perhaps important from a fundamental viewpoint, they hold no promise of scale-up as a viable commercial energy source. However, the claim of Fleischmann, Pons, and Hawkins[1] (FPH) involves large and easily detectable levels of excess power and nuclear fusion products. It is to the latter report that this article is addressed.

FPH reported electrochemical experiments that resulted in the generation of excess heat, tritium, and neutron emission.[1] They concluded that the rate of excess heating and the presence of typical fusion products could only be accounted for by invoking a heretofore unknown nuclear fusion process since the quantity of fusion products detected was many orders of magnitude lower than expected on the basis of the claimed power output. The reports from FPH have centered on the generation of excess heat in electrochemical cells containing Pd cathodes, Pt anodes, and LiOD/$D_2O$ electrolyte solutions, operated at current densities in the range 8–512 mA/cm$^2$ and at voltages between 2–10 V. The FPH radiation measurements have been critiqued by some of us previously,[4] and found to contain serious omissions and inaccuracies. As a result of this analysis, the γ-ray spectroscopic results have been retracted by Fleischmann,[5] and later reasserted[6] along lines which still contain equally fundamental errors.[4b] At present there are two additional reports[7,8] which corroborate the level of excess heating reported by FPH, and one report of fusion products.[9] Importantly, there has been no report of excess heat generation correlated with observation of fusion products from the same cell despite efforts to exactly replicate the FPH experiment. Modifications to the FPH

[1] Department of Chemistry, Massachusetts Institute of Technology, Cambridge, Massachusetts 02139.
[2] Plasma Fusion Center, Massachusetts Institute of Technology, Cambridge, Massachusetts 02139.
[3] Department of Nuclear Engineering, Massachusetts Institute of Technology, Cambridge, Massachusetts 02139.
[4] Department of Materials Science and Engineering, Massachusetts Institute of Technology, Cambridge, Massachusetts 02139.
[5] Authors to whom correspondence should be addressed.



0164–0313/90/0600-0133$06.00/0 

experiment intended to enhance the reported effects have similarly failed to yield excess heat or fusion products.[10] In addition to research activity among experimentalists there has been considerable effort directed toward a theoretical understanding of processes that might be responsible for cold fusion, but the consensus has generally been negative.[10–13]

The purpose of our investigation is to replicate as nearly as possible the experimental procedure of FPH. Accordingly, we have used information from the refereed scientific literature[1,6] or presented by FPH at scientific meetings in designing our experiments.[14,15] Furthermore, in determining what represents relevant evidence for nuclear fusion, we have focused our measurements and analyses on D-D fusion branches (Table I, Eq. A-C).[16] However, our measurements are sensitive to fusion products generated by all of the reactions shown in Table I except Eq. (F).

At high temperatures, Eqs. (A and B) (Table I) have branching ratios of about 50%,[16] while Eq. (C) is suppressed by $\sim 10^7$. These branching ratios are energy-dependent and may not apply to fusion reactions at low energy, although similar results have been measured for low energy, muon-catalyzed fusion.[17] Fleischmann[15] has suggested that Eq. (C) might be enhanced in cold fusion, and that it could be responsible for the presence of excess power in the absence of commensurate levels of neutrons and tritium.

The first phase (Phase I) of these experiments was begun shortly after the announcement of cold fusion by FPH. Because of the limited time available for implementation of Phase I, the techniques and error limits were relatively crude. Nevertheless, the level of sensitivity was sufficient for detecting the magnitude of excess power and neutron emission claimed by FPH. Phase I experiments are summarized in Section 4.

The second phase (Phase II) of the investigation featured improved accuracy and data acquisition, and a more thorough analysis of the Pd cathodes, electrolyte solutions, and effluent gases for fusion products. The cells were analyzed by the following means: (1) constant temperature calorimetry, (2) neutron counting and $\gamma$-ray spectroscopy, (3) mass spectral analysis of $^4$He in effluent gases, and $^4$He and $^3$He within the Pd lattice, (4) tritium analyses of the electrolyte solutions, and (5) x-ray photoelectron spectroscopy of the Pd cathode surface.

Within our estimated levels of accuracy, which are given in individual sections of this report, we found no evidence of any excess power output, fusion products, or any other evidence of nuclear fusion occurring in electrochemical cells modeled after those described by FPH.[1,14,15]

**Table I.** Nuclear Fusion Reactions[a]

| Reaction | Equation |
|---|---|
| A | D + D → n [2.45 MeV] + $^3$He [0.82 MeV] |
| B | D + D → H [3.02 MeV] + T [1.01 MeV] |
| C | D + D → $\gamma$ [23.8 MeV] + $^4$He [0.08 MeV] |
| D | D + $^6$Li → n [2.96 MeV] + $^7$Be [0.43 MeV] |
| E | D + $^6$Li → $^4$He [11.2 MeV] + $^4$He [11.2 MeV] |
| F | D + $^6$Li → H [4.39 MeV] + $^7$Li [0.63 MeV] |
| G | D + $^7$Li → n [13.36 MeV] + $^8$Be [1.67 MeV] → n [13.36 MeV] + $^4$He [0.85 MeV] + $^4$He [0.85 MeV] |
| H | D + $^7$Li → $\gamma$ [16.7 MeV] + $^9$Be [0.02 MeV] |
| I | D + $^7$Li → p + $^8$Li (endoergic, −1.01 MeV) → → p + $^4$He [8.05 MeV] + $^4$He [8.05 MeV] |
| J | D + $^7$Li → T + $^6$Li (endoergic, −1.81 MeV) |

[a] From Ref. 16.

## 2. SOLID STATE CHEMISTRY OF Pd

The absorption of H or D by metallic Pd has been extensively investigated.[18,19] The face-centered cubic Pd host lattice expands as H or D atoms begin occupying octahedral sites and forming $PdH_n$ or $PdD_n$ solid solutions.[20] Recent theoretical calculations of the structure of H or D in Pd clusters[21] and in bulk Pd[22] suggest that even at the very high H or D concentrations postulated to exist in $PdD_2$, the equilibrium distance between two D atoms is ~0.2 Å larger than the $D_2$ intramolecular spacing of 0.74 Å.[22]

Below 300 °C, the $PdH_n$ or $PdD_n$ homogeneous solid solution can exist in two phases: a hydrogen-poor $\alpha$ phase and a hydrogen-rich $\beta$ phase. Values for the maximum H/Pd ratio at which the $\alpha$ phase can exist, $\alpha_{max}$, and for the minimum H/Pd ratio necessary to form the $\beta$ phase, $\beta_{min}$, are $\alpha_{max} = 0.008$ and $\beta_{min} = 0.607$ at 25°C.[19] At $T = 25$°C and $P = 1$ atm, the maximum H/Pd loading ratio which can be achieved by gas charging is about 0.7.[23] Electrolytically-prepared hydrides with H/Pd loading ratios as high as 0.9 have been reported, however these materials are unstable at ambient conditions and slowly lose hydrogen upon standing.[23] In practice, the maximum D/Pd ratio that can be obtained by electrolysis of $D_2O$ varies with the conditions of the electrolysis and on the pretreatment of the Pd cathode. However, for cathodes which have been equilibrated with air at $T = 25$°C and $P = 1$ atm, a value in the range D/Pd = 0.7–0.8 is widely accepted.[19] It has been es-

timated that the flux of H into Pd upon electrolysis of $H_2O$ is $\sim 10^{16}$ molecules/cm$^2$-s (p.37).[19] Based on this value and the dimensions of the Phase II Pd cathodes (Table II), we can roughly calculate the loading time for the electrodes (D/Pd ~0.7) to be about 33 h.

To ascertain a lower bound on the loading factor reached at the end of the Phase II experiments, the Pd cathodes were degassed by heating and the evolved gas collected. Under the conditions of degassing ($T$ = 260°C, $P$ = 1 atm), the ratio H/Pd is known to fall to ~0.02 (p. 22).[19] The Pd rods were heated until degassing ceased, about 1 h, and the loading factors were calculated based on the volume of gas expelled, and independently by the change in weight of the Pd rods. The average loading ratios were found to be 0.75 ± 0.05 and 0.78 ± 0.05 for the D and H loaded cathodes, respectively. These values indicate that during Phase II experiments, the cathodes were loaded with D or H near the maximum level, and were well into the Pd β phase. Similar analyses of some Phase I rods indicated slightly lower D/Pd loading in the range 0.6–0.7.

In addition to absorbing hydrogen isotopes, electrolytic Pd/$D_2O$-electrolyte solutions exhibit an inverse isotope effect. That is, the higher mass isotopes will concentrate in the liquid phase relative to either the gas or solid phase.[24,25] Therefore, upon extended electrolysis in $D_2O$ electrolyte solutions in which hydrogen and tritium are present at low concentration, the solution phase will become enriched in the heavier isotopes and the Pd cathode will become enriched in the lighter isotopes. When determining the tritium content of cells thought to be generating tritium by nuclear processes, the presence of tritium above the background level may only indicate preferential concentration of tritium in the solution by the normal separation process described previously.

**Table II.** Phase II Cell Parameters

| | $H_2O$ Cell | $D_2O$ Cell |
|---|---|---|
| Cathode | Pd Rod<br>0.1 × 9 cm | Pd Rod<br>0.1 × 9 cm |
| Anode | Pt wire<br>0.5 × 70 cm | Pt wire<br>0.5 × 70 cm |
| Electrolyte | 0.25 M LiOH/$H_2O$ | 0.25 M LiOD/$D_2O$ |
| Volume | 55 mL | 55 mL |
| Current | 196 ± 2 mA | 195 ± 2 mA |
| Current density | 69 mA/cm$^2$ | 69 mA/cm$^2$ |
| Voltage | 2.86 ± 0.03 V | 2.88 ± 0.03 V |
| Start time | 4/20/89 (9:45 h) | 4/20/89 (18:30 h) |
| Stop time | 4/29/89 (16:15 h) | 4/29/89 (16:15 h) |
| Duration | 223 h | 213 h |

## 3. PREPARATION OF ELECTRODES AND ELECTROLYTE SOLUTIONS

A Pd (99.96%) rod (0.64 × 10 cm) (Johnson Matthey/Aesar, Seabrook, NH) was cut into four 2.5-cm-long sections and used in Phase I experiments (Table III). Pd wire 0.1 cm in diameter (Engelhard, Iselin, NJ) was used in the remaining Phase I experiments and in Phase II. The pre-treatment of Phase I cathodes is shown in Table III. Phase II cathodes were degassed by heating to 725°C in vacuum prior to use. Pt (99.99%) anodes were fashioned from 0.1-cm wire (Johnson Matthey/Aesar, Seabrook, NH).

The $D_2O$/LiOD electrolyte solutions were prepared by addition of LiD powder (98% D; Alfa Products, Danvers, MA) to $D_2O$ (Phase I: 99.9% D, lot number F11G; Phase II: 99.8% D, lot number F7962; Cambridge Isotope Laboratories, Medford, MA) under an inert atmosphere. The $H_2O$/LiOH electrolyte solutions were prepared by mixing glass distilled $H_2O$ (EM Science, Cherry Hill, NJ) and LiOH (Alfa Products, Danvers, MA) in air.

Specific experimental details relating to calorimetry, nuclear measurements, and the assays of fusion products are reported in individual sections.

## 4. PHASE I EXPERIMENTS

The Phase I experiments were begun within a few days of the announcement of cold nuclear fusion. The hastily assembled Phase I apparatus allowed simple calorimetry, neutron counting, and γ-ray spectroscopy.

The single compartment glass cells were suspended in air and contained $D_2O$/0.1 M LiOD, Pd rod cathodes, and helically-wound Pt wire anodes (~0.1 × 20 cm) mounted coaxially with the Pd cathode. Gases generated during electrolysis were vented through a mineral oil bubbler fitted with a drying tube to prevent contamination of $D_2O$ by atmospheric $H_2O$. The Pd cathode pretreatment, duration of electrolysis, electrolyte concentration, and range of current densities are shown in Table III. The measured D/Pd loading factor in the cathodes tested was ~0.62 ± 0.05 indicating these cathodes were in the Pd β phase.

Cell temperature was monitored by continuously recording the voltage of a chromel-alumel thermocouple in thermal contact with the exterior wall of each cell. The relationship between temperature and power was

**Table III.** Phase I Cell Parameters

| Cell electrode size (cm) | Electrolyte | Start (m/d/y) | Stop (m/d/y) | Electrode preparation | Current density range (mA/cm²)[a] |
|---|---|---|---|---|---|
| A 0.64 × 2.5 | 0.1 M LiOD | 3/27/89 | 5/19/89 | Solvent rinse | 35–175 |
| B 0.64 × 2.5 | 0.1 M LiOD[b] | 3/27/89 | 5/19/89 | Solvent rinse | 35–175 |
| C 0.10 × 2.5 | 0.1 M LiOD | 3/28/89 | 4/19/89 | Solvent rinse | 64–950 |
| E 0.64 × 2.5 | 0.1 M LiOD | 3/28/89 | 4/7/89 | 700°C/vacuum | 35 |
| F 0.64 × 2.5 | 0.1 M LiOD | 4/1/89 | 5/19/89 | 700°C/vacuum | 40–280 |

[a] The current density was periodically varied between these limits for the duration of the experiment.
[b] 2 M $LiNO_3$ added after 3 days.

calibrated by inserting a 15-ohm resistor into the cell and recording the temperature rise as a function of electrical power dissipated in the resistor. The calibration was nearly linear over the temperature range of interest and had a slope of 0.2 W/°C. Variations in cell temperature of 1.5 °C were easily detectable, making the resolution of the Phase I calorimeter ~0.3 W. For 0.4 × 10-cm Pd rod cathodes operating at 64 mA/cm² FPH reported an excess power of 1.4 W/cm³.[1] Based on the volume of the Phase I electrodes, and assuming similar excess power gain for these slightly larger diameter cathodes, we expected to observe at least 1.1 W of excess power, a value within the resolution of our calorimeter. However, over the course of the Phase I experiments we did not observe any changes in cell temperature except those related to changes of input power level, electrolyte volume, ambient temperature, and other experimental variables.

Neutron emission was measured using a moderated $BF_3$ detector which was absolutely calibrated with a Pu/Be source emitting $1.5 \times 10^6 \pm 6 \times 10^4$ n/s.[26] During calibration the geometry of the source relative to the Phase I detector, $D_n1$, closely approximated that of the electrochemical cells and detector. The measured background rate of the detector was 0.7 ± 0.02 cts/min which is equivalent to a source strength of 216 n/s at a distance of 1 m between the source and the detector; in Phase I, this distance ranged from 30 cm to 1 m. For the closest cell, the minimum detectable neutron source rate would have been 19 n/s. FPH[1] have reported the rate of neutron emission from their cells as $3.2 \times 10^4$ n/s-cm³ for a 0.4 × 10 cm Pd rod operated at 64 mA/cm². Normalized to the volume of the Phase I Pd cathodes this corresponds to a source strength of $\sim 2.6 \times 10^4$ n/s, or about $1 \times 10^2$ above the background level. Accordingly, the level of neutron emission from any "fusing cell" is easily within the detection limit of $D_n1$.

Figure 1 shows the $BF_3$ detector counting rate measured during a period of 10 days commencing at the beginning of the electrolysis of cells C and E. The average neutron count rate during the time that the cells operated was 0.7 cts/min. This rate was identical to the background count rate measured after electrolysis was stopped and the cells removed from the room where the experiments took place. Neutron measurements were continued until all cells were disconnected, but throughout this time the background count rate always equaled the average count rate.

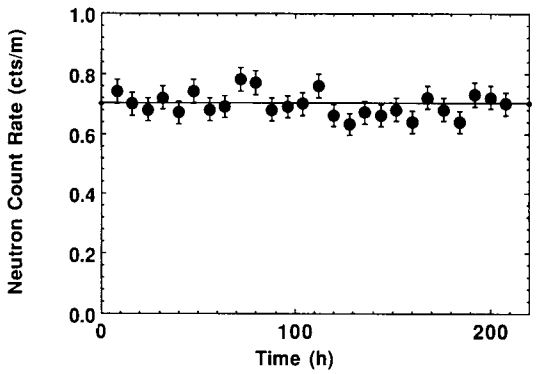


**Fig. 1.** Neutron count rates during Phase I experiments detected using a moderated $BF_3$ detector ($D_n1$). Each point corresponds to an 8-hour average. The geometry and efficiency of the detector is described in Section 4.

FPH[1] originally reported observation of 2.22-MeV γ-ray line originating from neutron-capture-on-hydrogen (Eq. 1).

$$n + p \rightarrow D + \gamma\ [2.22\ \text{MeV}] \qquad (1)$$

They contended that the neutron radiation in their experiment was generated according to Eq. (A) (Table I). More recently, FPH[6] have suggested that their γ-ray peak actually resides at 2.5 MeV, and is not due to

neutron-capture-on-hydrogen. However, they are unable to assign this feature to a nuclear process or to account for its unphysical shape.[4b] We measured the γ-ray spectrum in the vicinity of our electrochemical cells with a 3 in × 3 in NaI (Tl) crystal spectrometer system over the ranges 0–3 MeV and 0–30 MeV. Water was interposed between the cells and the spectrometer to thermalize the neutrons and permit observation of γ-rays generated according to Eq. (1). A complete description of the spectrometer, calibration procedure, and an analysis of the FPH data are given in Sections 7 and 10. The important result is that during Phase I experiments, no spectral features were detected in the γ-ray spectra except those corresponding to background processes.

FPH[1] reported the presence of tritium in electrochemical cells generating excess power which they ascribed to the presence of a nuclear fusion reaction (Eq B, Table I). We also searched for tritium by periodically removing 1–2 mL samples of electrolyte from Phase I cells and analyzing by a procedure detailed in Section 8.2. However, we did not detect a level of tritium significantly above the measured background level of 300 ± 50 dpm/mL in Phase I cells at any time during electrolysis.

In summary, we analyzed cells modeled after those described by FPH for excess power, neutron and γ-ray emission, and tritium content. Our error limits in all cases would have permitted us to detect the magnitude of changes FPH have contended occur in cells undergoing cold fusion. However, in Phase I experiments, we were unable to reproduce the effects reported by FPH, and we did not observe any evidence for excess power generation or any other nuclear fusion processes.

## 5. PHASE II CELL AND CALORIMETER CONFIGURATIONS

### 5.1. Electrochemical Cell

The cell used for Phase II experiments is shown in Fig. 2a. This design was chosen because it is essentially the same as that employed by FPH.[1] A Pd cathode is supported in the center of the cylindrical Pyrex cell by two Teflon guides. Electrical contact to the cathode was achieved by spot welding a length of Teflon-wrapped Pt wire to the top of the Pd cathode. The Pt anode and a Teflon-coated nichrome heating element are wound helically around two concentric rings of Pyrex tubes. This configuration provided a distributed, axially-symmetric heat source and reduced thermal gradients in solution compared to systems using small asymmetrically-disposed heating elements. Two tubes in the inner ring, which support the anode, serve as feedthroughs for the temperature monitors. The heater feedback was monitored by a Pt RTD thermometer accurate to 0.1°C (Omega Engineering, Stamford, CT) enclosed in a thin-walled glass tube filled with mineral oil to ensure good thermal contact between the RTD thermometer and the electrolyte solution. The temperature of the cell was monitored by a similarly configured chromel-alumel thermocouple.

The cell was filled with electrolyte solution to a level several centimeters above the top of the upper Teflon support. This ensured that the Pd cathodes, which can act as a $D_2/O_2$ or $H_2/O_2$ recombination catalyst, would not be directly exposed to gas in the cell headspace. In addition, this extra volume reduced the need for frequent additions of solvent to replenish that which evaporated or was electrolyzed. As described in Section 6, we found that correction for steady power drifts caused by loss of solvent was possible, but that frequent additions of fresh solvent appeared to cause a decrease in cell power which was more difficult to account for.

Additional holes present in the Teflon supports permitted outflow of the electrolysis gases. However, these holes did not completely eliminate the formation of large bubbles within the cell. Gases were permitted to leave the cell through a mineral oil bubbler vented through a drying tube to prevent contamination of the $D_2O$-containing electrolyte by atmospheric $H_2O$. $D_2O$ or $H_2O$ was added to the cells by injection through a gas tight rubber septum. The cell was placed in a glass jar containing glass wool to reduce thermal convection and ensure a fixed thermal transport rate from the cell into the surrounding constant temperature bath.

### 5.2. Calorimeter

Phase II experiments utilized a constant temperature calorimeter having a sensitivity of about 40 mW. Constant cell temperature was maintained using a temperature feedback control system connected to the heating element (Fig. 2b). Power fluctuations generated in the cell were detected as changes in the applied heating power. In operation, the temperature signal was compared to a reference setpoint and a correction signal was generated proportional to the difference between the setpoint and the cell temperature. The correction signal was amplified and used to drive a heating element. The cell operating temperature, $T_c$, was typically 46°C.

During experimental runs the following cell parameters were continually monitored: $T_c$; bath temperature,

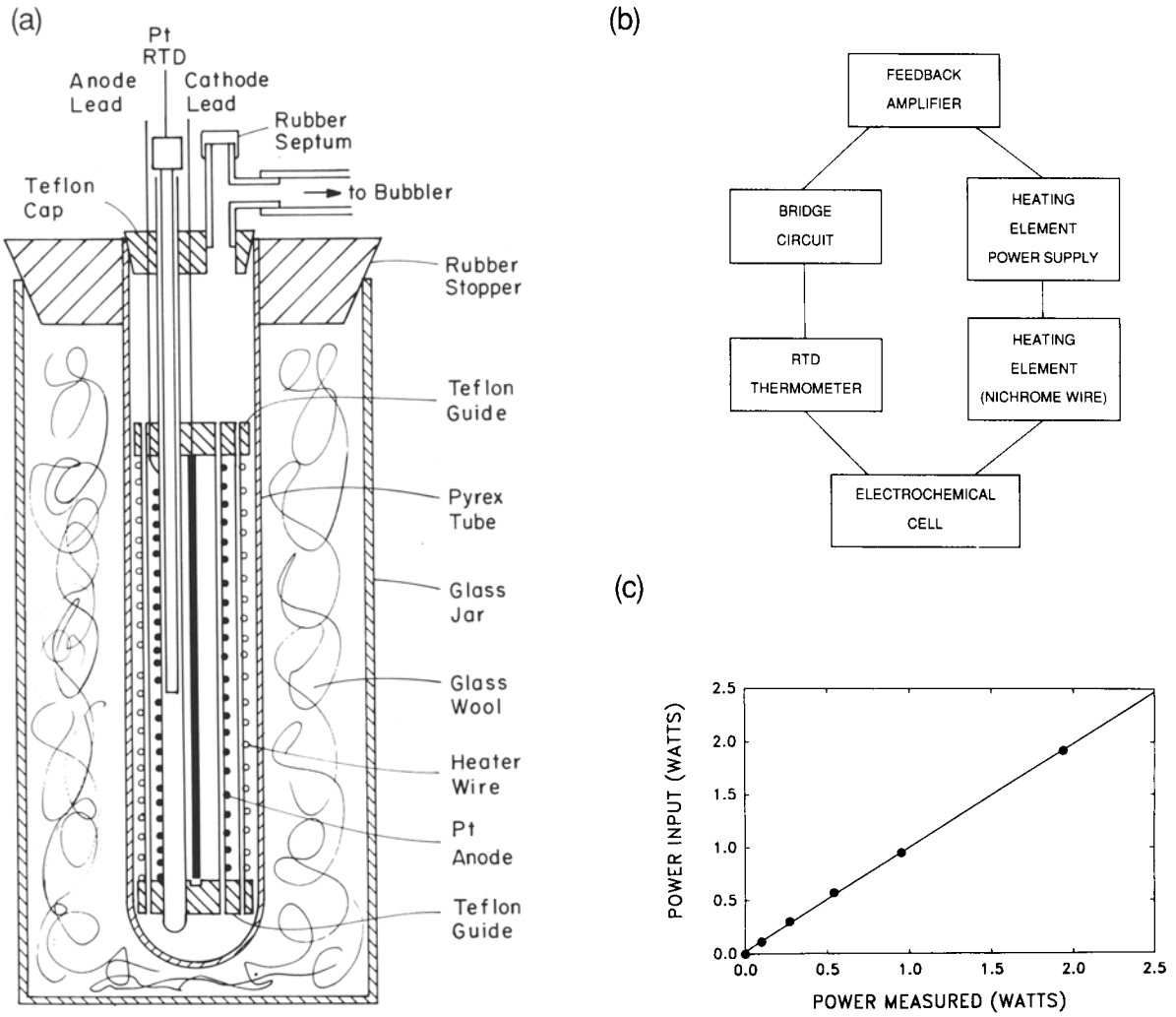


**Fig. 2.** Phase II calorimeter. (a) Cross-sectional view of the Phase II cell. The cell height is about 12 cm. (b) Block diagram of the logic of the feedback control system. (c) Test calibration of the calorimeter. The power input to the cell from a standard resistive heat source is plotted against power measured with the constant temperature calorimeter. The input power is accurate within 3%.

$T_b$; cell voltage and current, $V_c$, $I_c$; and heater voltage and current, $V_h$, $I_h$. The data were A/D converted with a multiplexed Hewlett-Packard auto-ranging high precision digital voltmeter, and the thermocouple was referenced to an electronic reference junction. All resulting digital data were stored on disk at a sample period of, typically, 120 s.

## 6. PHASE II POWER MEASUREMENTS

Under steady state, isothermal conditions the input power to the cell consisted of the cell power, $P_c = I_c V_c$, the heater power $P_h = I_h V_h$, plus any unknown anomalous power in the cell, $P_x$. Power was lost from the cell through two dominant channels, thermal transport, $P_{th}$, and loss of the electrolysis products $H_2$ (or $D_2$) and $O_2$, $P_e$. Thermal transport to the external constant temperature bath took place through a layer of dead air space packed with glass wool and to a lesser extent to the ambient atmosphere through the top of the cell. Evolution of the reaction products, $D_2$ and $O_2$, consumed power at a rate given by $P_e = V_e I_c$, where $V_e$ is the potential associated with the enthalpy change of the electrolysis of water. Recombination of the gaseous products will effectively reduce $P_e$, and is a significant source of error

for calorimetry in open cells when the degree of recombination is not measured. Under steady state conditions the cell power balance equation is given by Eq. (2).

$$P_h + P_c + P_x = P_{th} + P_e \quad (2)$$

If thermal gradients in the cell are sufficiently small (a discussion follows), and if recombination is negligible, then at constant $I_c$ and $V_c$, Eq. (2) reduces to Eq. (3).

$$P_x + P_h = \text{constant} \quad (3)$$

This equation allows the unknown power, $P_x$, to be determined. If $P_x$ increases, then the feedback control system of the calorimeter reduces $P_h$ to maintain $T_c$ constant.

As a test of our calorimetric method we measured the values of $V_e^{D_2O}$ and $V_e^{H_2O}$. In this experiment, $T_c$ was brought to its normal operating value by application of only $P_h$. When the electrolysis was switched on, $P_h$ decreased to compensate for the power due to Joule heating, $P_c - P_e$, which is always present in electrochemical cells. By application of Eq. (4),

$$P_h^o = P_h^f + [P_c - (V_e \times I_c)] \quad (4)$$

where $P_h^o$ and $P_h^f$ are the heater powers before and after the electrolysis is turned on, we can experimentally determine $V_e$. The results of this experiment gave $V_e^{D_2O} = 1.57$ V and $V_e^{H_2O} = 1.41$ V, compared to the theoretical values which are 1.53 V and 1.48 V, respectively.[27] This measurement indicates that short time scale changes in $P_x$ can be detected with ~5% accuracy.

A significant source of error in calorimetric measurements is the formation of thermal gradients in the cell. For the cell design shown in Fig. 2a, streaming of small gas bubbles formed as a result of electrolysis caused sufficient mixing to eliminate thermal gradients. However, when the cell current density was reduced below ~18 mA/cm$^2$ detectable errors in the cell power balance appeared. In all of the experiments reported here, current densities higher than 18 mA/cm$^2$ were used. A test of the calorimeter calibration was carried out at $I_c = 0$ using a heating element immersed in the cell. To eliminate thermal gradients during this testing, $N_2$ was bubbled into the bottom of the cell at a rate intended to simulate electrolytic bubbling. Calibration tests using the standard heat source were found to be accurate to within 3% as shown in Fig. 2c.

To test for the presence of anomalous power generation in $D_2O$-containing electrolyte solutions as compared to $H_2O$-containing electrolyte solutions, the two Phase II cells described in Section 5 were run for approximately 200 hours under galvanostatic conditions (Table II). The cell parameters, $I_c$, $T_c$, $V_c$, and $P_h$ are shown for a 1.2-h period near the end of the run (Fig. 3). The data for $P_h$ indicate that there is no significant difference in heat generation between the $D_2O$ cell and $H_2O$ cell to within the 40-mW sensitivity of the calorimetry. Moreover, no excess power was found in any of the cells. The excess power claimed by FPH[1] for 0.1-cm diameter cathodes at 64 mA/cm$^2$ would be about twice the sensitivity of our calorimeter and if present would have been detectable.

The comparison experiment described took place over a short period in comparison to the time scale of evaporation and electrolytic decomposition of the solvent. Data which demonstrates the long-term stability of the Phase II parameters, $I_c$, $V_c$, and $T_c$, are shown in Figs. 4a and 5a. However, measurement of $P_h$ over a 100-h period (Fig. 6) indicates a significant drift caused by the reduction of solvent volume. We demonstrated that this drift was due to solvent loss rather than to an unknown power source, $P_x$, by calibrating $P_{th}$ as a function of electrolyte solution volume. When enough solvent was added to the $D_2O$ cell to compensate for that lost to electrolysis at the end of the 100-h period shown in Fig. 6, $P_h$ returned to within 20% of its original value. If the total volume of solvent lost over the course of the experiment had been taken into account, including that lost to evaporation, $P_h$ would have been even closer to its original value.

In addition to the steady drift, a high frequency

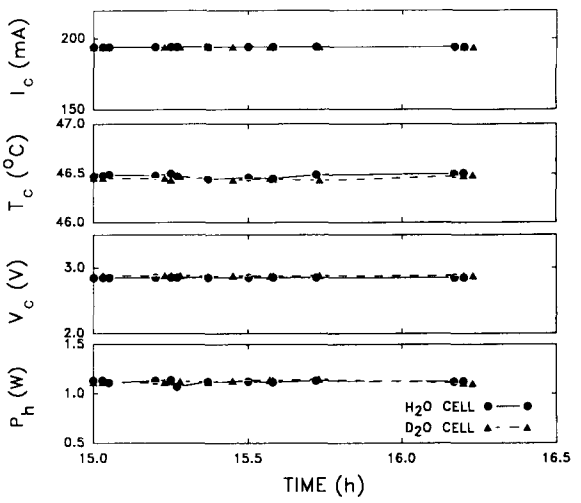


**Fig. 3.** Time history of the Phase II cell current, $I_c$; temperature, $T_c$; voltage, $V_c$; and heater power, $P_h$; during a 1.2-h period after approximately 200 h of electrolysis.

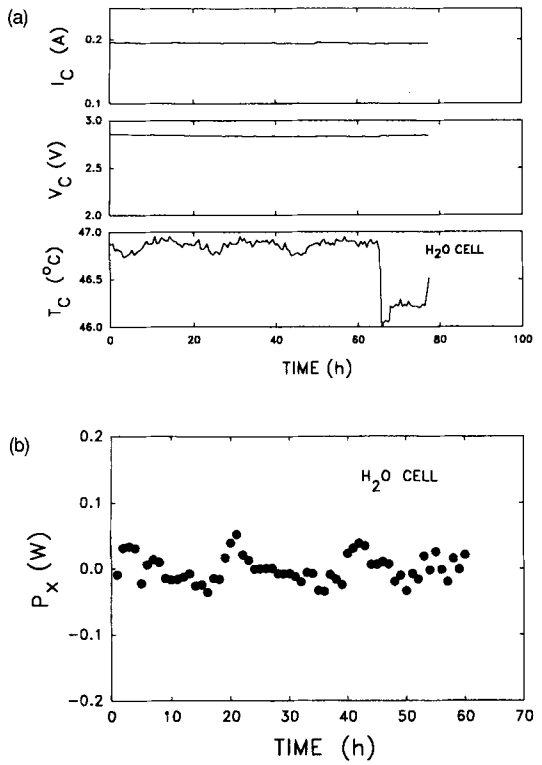


**Fig. 4.** (a) Time history of the cell current, $I_c$; voltage, $V_c$; and temperature, $T_c$, for the Phase II $H_2O$ cell (22:00 h, 4/25/89–04:00 h, 4/29/89). At 65 h, the set point for the cell temperature was changed from 46.8°C to 46.2°C. (b) Time history of the "anomalous" power, $P_x$, in the $H_2O$ cell. These data have been time averaged over 1-h blocks. The baseline drift caused by solvent loss has been subtracted.

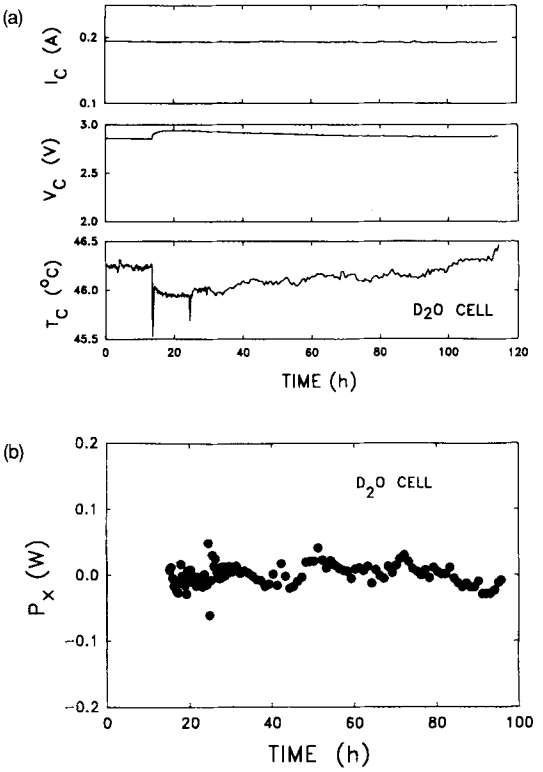


**Fig. 5.** (a) Time history of the cell current, $I_c$; voltage, $V_c$; and temperature, $T_c$, for the Phase II $D_2O$ cell (8:00 h, 4/23/89—3:00 h, 4/28/89). At 15 h, the set point for the cell temperature was changed from 46.7°C to 46.0°C. (b) Time history of the "anomalous" power, $P_x$, in the $D_2O$ cell. These data have been time averaged over 1-h blocks. The baseline drift caused by solvent loss has been subtracted.

component was also observed in $P_h$. The magnitude of the high frequency oscillation decreased significantly when the electrolysis reaction was turned off. The long-time variation of $P_h$ can best be seen by smoothing the high frequency oscillations using digital filtering, and correcting the sloping baseline by fitting the drift with a linear function and subtracting from the signal (Figs. 4b and 5b). The data show a slowly fluctuating power level in both the $H_2O$ and $D_2O$ cells, but neither show evidence of sustained power production at the levels claimed by FPH.[1] For the current density used here, FPH reported a power level of 79 mW, a level above the fluctuation level present in Figs. 4b and 5b. The low level power fluctuations apparent in Figs. 4b and 5b may be caused by a number of processes, for example, gas recombination, bubble trapping, or droplet formation. These effects are discussed in Section 11.

## 7. RADIATION MEASUREMENTS

### 7.1. Neutron Measurements

The Phase I neutron detector, $D_n1$, was discussed in Section 4. This detector was operated in a similar configuration in Phase II, however an additional detector, $D_n2$, was also present and integrated into the computer data acquisition system. $D_n2$ was calibrated with the source described in Section 4 and was found to be somewhat less sensitive than $D_n1$. For $D_n2$, the average count rate recorded was 0.8 cts/min (Fig. 7), which corresponds to a minimum detectable source rate of 42 n/s at the nearest cell (20 cm) and to $10^3$ n/s at the farthest one (100 cm). $D_n1$ was recalibrated using a smaller distance between the source and the detector, however, the average background count rate did not change from that found in Phase I, 0.7 cts/min. This corresponds to a

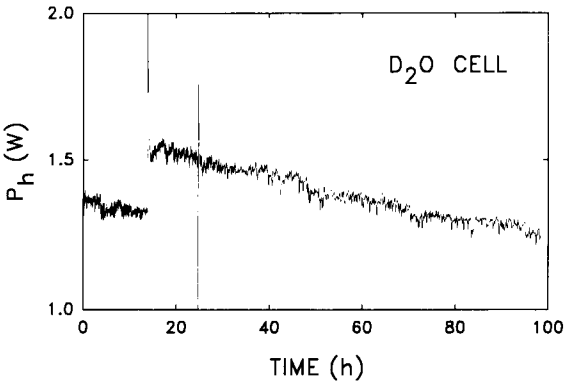


**Fig. 6.** Time history of the calorimeter heater power over a 100-h period of electrolysis for the $D_2O$ cell (8:00 h, 4/24/89—12:00 h, 4/28/89). The increase in $P_h$ at 16 h into the run was caused by addition of 5 mL of $D_2O$ to the cell, and the fluctuation 8 h later was intentionally introduced as a time calibration mark. At 30 h, the rate of data acquisition was reduced and the trace appears lighter.

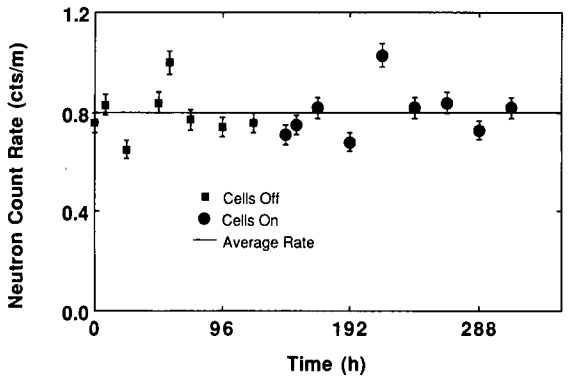


**Fig. 7.** Neutron count rates before and during Phase II experiments detected using a moderated $BF_3$ detector ($D_n2$). Each point corresponds to an 8-hour average. The geometry and efficiency of the detector is described in Section 7.1.

minimum detectable signal of 60 n/s from cells which were typically 37 cm from the detector.

The neutron rate reported by FPH was $3.2 \times 10^4$ n/s-cm$^3$. A neutron rate of this magnitude would have appeared on $D_n2$ as a count rate of between 40–1000 times background level, and 650 times background on $D_n1$. Such signals would have been easily observable, yet no increase in signal above background occurred in either phase of our experiment. While the neutron detectors used were somewhat insensitive and would not have been capable of making a measurement at the level reported by Jones,[2] they were more than adequate to measure an effect as large as that reported by FPH.[1,6]

### 7.2. γ-Ray Measurements

The gamma radiation was monitored by two 3 in × 3 in NaI(Tl) scintillation detectors. Detector 1, Dγ1, covered the energy range from 0–3 MeV for measurement of the purported 2.22-MeV neutron-capture-on-hydrogen γ-ray. Detector 2, Dγ2, covered the energy range from 0–30 MeV for measurement of the 23.8-MeV γ-ray from Eq. (C) (Table I). The two detectors were located underneath the water tank containing the electrolysis cells, and were collimated with about 10 cm of lead shielding. The detectors viewed the cells through approximately 5 cm of water and 1 cm of plastic. The γ spectra were stored continuously in RAM and dumped to disk every 100 minutes.

The sensitivity of Dγ1 to the neutron-capture γ-rays was experimentally measured with a $1.5 \times 10^6$ n/s (Pu/Be) neutron calibration source placed in the center of the water tank. The measured gamma rate was about 1700 cts/MeV-s at 2.22 MeV (Fig. 8a). Given the background rate of 0.7 cts/MeV-s at this energy (Fig. 8b), the minimum detectable rate was about 200 n/s. The sensitivity of Dγ2 to 23.8 MeV photons was estimated based on the background γ-rate, the detector efficiency, and the detector geometry. For the background rate of 0.02 cts/MeV-s at 23.8 MeV (Fig. 9), and for a detector efficiency of ~50% for these photons in a 3 in × 3 in NaI(Tl) crystal, the detector can measure a γ rate of ~10 photon/s generated in the cell.

After nearly 2 months of monitoring Phase I and Phase II cells, we observed no increase in the γ emission rate above the background level. This sets the upper limits on the rates of the reactions corresponding to Eqs. (A and C) (Table I) to be 200 reactions/s and 10 reactions/s, respectively. The maximum reaction rate sets an upper limit on excess power arising from Eq. (A) (Table I) of $\sim 10^{-9}$ W/cm$^3$ in Phase II cells. This value is significantly more sensitive than calorimetric power measurements, and suggests that the presence of γ radiation would be a more convincing indicator of nuclear fusion than calorimetric excess power measurements. Based on the maximum reaction rate for Eq. (C) (Table I), we can also set a maximum fusion power limit of $\sim 10^{-9}$ W/cm$^3$. However, this energy should not appear as heat in the electrochemical cell, barring a new mechanism that couples energy into the Pd lattice, since most of the energy would be carried off by the photon.

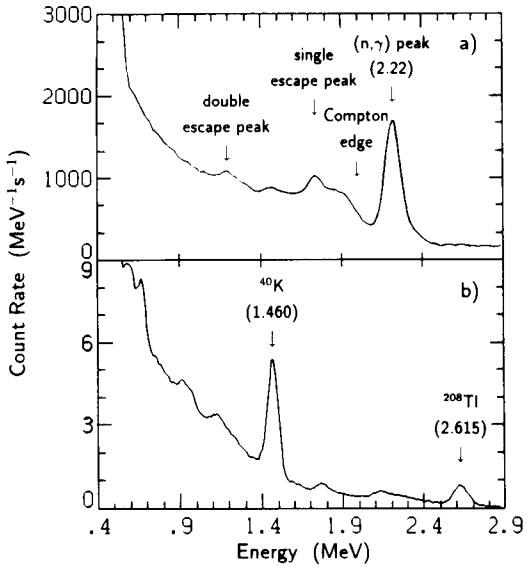


**Fig. 8.** γ-ray spectra measured with a 3 in x 3 in NaI (Tl) scintillation detector (Dγ1) covering the energy range 0–3 MeV. (a) A neutron-capture-on-hydrogen spectrum obtained with a 1.5 x $10^6$ n/s (Pu/Be) calibration neutron source submerged in water. Appearing are the (n,γ) peak (2.22 MeV), a Compton edge (1.99 MeV), and the first and second escape peaks. (b) Background γ-ray spectrum. The background γ-rate at 2.22 MeV is about 0.7 cts/MeV-s. Using the neutron-capture γ-ray experiment as a calibration, a 200 n/s source can increase the γ rate at 2.22 MeV by ~25% above the background.

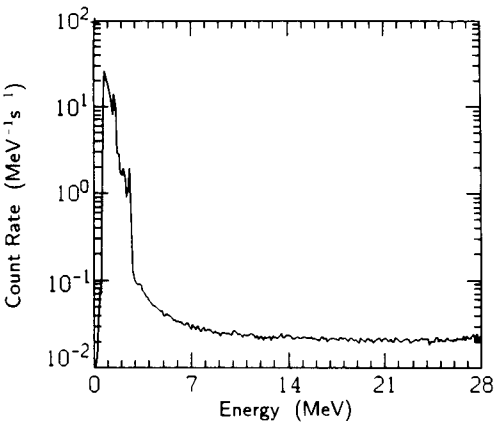


**Fig. 9.** A background γ-ray spectrum measured with a NaI (Tl) detector (Dγ2), covering the energy range 0–30 MeV. Based on the background γ-rate at 23.8 MeV, and for a ~50% detection efficiency for these γ-rays, the detector is sensitive to a γ rate of 10 photon/s from Phase II cells.

## 8. FUSION PRODUCT ANALYSIS

We have performed detailed experiments designed to detect the presence of fusion products generated in Phase II cells, because unambiguous detection of fusion products is a definitive test for cold fusion in Pd cathodes. Furthermore, the presence of fusion products is generally a more sensitive test for fusion power generation than the calorimetric methods described by us and others.[1,7,8] In this section, we will describe the results of experiments designed to detect fusion products in effluent gases, electrolyte solutions, and inside Pd cathodes.

### 8.1. Gas Phase

Electrochemical cells generating excess heat have been reported to evolve concentrations of $^4$He significantly higher than background levels.[28] Mass spectral analysis of gas evolved from Phase II cells was undertaken to detect the presence of $^4$He, a fusion product associated with Eqs. (C, E, and G) (Table I). Importantly, this analysis is only sensitive to fusion processes occurring on Pd surfaces, because the diffusion coefficient of He inside Pd is too low to permit internally-generated He to escape into the solution.[29]

A Finnigan MAT 8200 double-focusing, high resolution mass spectrometer was used for analysis of $^4$He and $D_2$ in the effluent gas of the electrolyzing Phase II cells. Gas samples were drawn with gas-tight syringes and injected into an evacuated glass tube attached to the inlet system of the high resolution mass spectrometer. The nominal resolution required to resolve the $^4$He and $D_2$ mass peaks, 4.0026 amu and 4.028 amu, respectively, is about 158. The resolution of our instrument was 500, sufficient to easily resolve the two mass peaks.

The data shown in Fig. 10 were taken over the mass range 3.9–4.1 amu. Figure 10a shows a spectrum of ambient air taken from the room where the cells were operated. Air samples taken from other locations showed the same peak magnitude, which we infer corresponds to the natural abundance of He in air, 5 ppm.[30] The result of a mass spectral analysis of the effluent gas from the electrolyzing Phase II $D_2O$ cell is shown in Fig. 10b. As expected for cells containing $D_2O$ the mass peak for $D_2$ is off-scale, however the height of the $^4$He peak is identical to that shown in Fig. 10a indicating that within our estimated detection limit, ~1 ppm above background, no excess $^4$He is produced in the electrolyzing cell.

It is possible to relate the fusion power level associated with Eq. (C) (Table I), to the detection limit of our $^4$He assay. Assuming all $^4$He is formed at the Pd surface, and using the energy released in Eq. (C) (Table

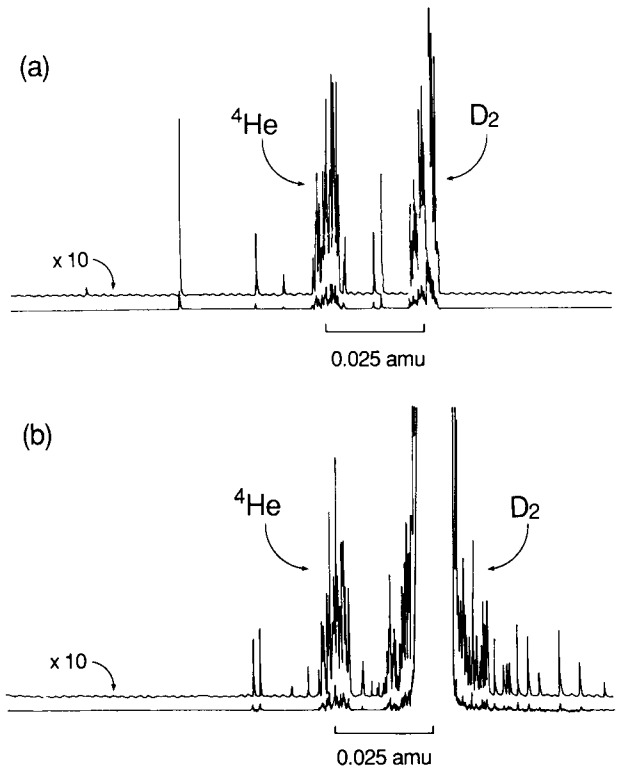


**Fig. 10.** Mass spectral analysis of gas samples taken from: (a) ambient laboratory air; (b) the effluent gas stream of an operating $D_2O$ cell. The mass range shown is from 3.9–4.1 amu. The peak height of $^4$He (4.0026 amu) is the same in both samples, ~5 ppm, indicating that no $^4$He above the background level is produced in the $D_2O$-containing cell.

I), and the rate of electrolysis (Table II), fusion power generation at a maximum rate of ~28 W/cm$^3$ could occur at the level of sensitivity of the $^4$He mass spectral assay. However, since most of the energy is carried off by the $\gamma$-ray, most fusion energy would not appear as heat in the cell.

## 8.2. Liquid Phase

Control and electrolyte samples were analyzed for tritium at the M.I.T. Radiation Protection Office using a Packard Model 2000 CA Liquid Scintillation Counter. 1 mL of sample was added to 10 mL of Packard Opti-Fluor scintillation fluid (Packard Instrument Co., Grove, IL). The samples were dark-adapted for 1 hour, and then each sample was counted for 2 min. Calibration was achieved by means of a quench correction curve using tritium standards of known concentration. The minimum detectable tritium level was 40 dpm/mL. Results for samples from Phase II experiments are given in Table IV.

The background tritium level in the $D_2O$ used for Phase II experiments was specified by the manufacturer to be less than 5 $\mu$Ci/kg which corresponds to $1.9 \times 10^{-10}$ M tritium or $1.2 \times 10^4$ dpm/mL. The experimentally-determined background level of tritium corresponded to ~100 dpm/mL. Analysis of the electrolyte solution from Phase II $H_2O$- and $D_2O$-containing cells showed no significant increase in tritium concentration after more than 200 hours of electrolysis (Table IV).

It is possible to relate the magnitude of fusion power which would be dissipated as heat in Phase II cells by Pd electrodes undergoing fusion according to Eq. (B) (Table I) to the concentration of tritium present in the electrolyte solutions. However, the accuracy of such an analysis is limited in open cells, since some atomic tritium may catalytically react and form molecular tritium, DT or $T_2$, at the Pd electrode surface rather than exchange with $D_2O$ to form TDO. Nevertheless, we can use the half life of tritium and the cell parameters listed in Table II to estimate the power released by the tritium branch of D-D fusion for our detection sensitivity. In closed cells, this calculation sets the maximum fusion power limit for Eq. (B) (Table I) at ~$10^{-7}$ W/cm$^3$. However, in our open cells, tritium may be lost prior to the assay and the actual power level could be higher, underscoring the advantages of using a closed cell configuration.

## 8.3. Solid Phase

If He were formed by a nuclear fusion process (Eq. C, Table I), it would be immobilized in the Pd metal. Experiments designed to measure the diffusion coefficient of He in $PdT_n$ have verified that diffusion in that medium is negligible as well.[29] Detection of a signifi-

**Table IV.** Phase II Tritium Data

| Sample | Scintillations (dpm/mL) |
|---|---|
| $H_2O$ | 45 ± 9 |
| $H_2O$/0.25 M LiOH | |
| Before electrolysis | 73 ± 7 |
| After 223 h electrolysis[a] | 63 ± 10 |
| $D_2O$ | 111 ± 17 |
| $D_2O$/0.25 M LiOD | |
| Before electrolysis | 101 ± 11 |
| After 214 h electrolysis[a] | 138 ± 16 |

[a]See Table II.

cant level of He in the metal would constitute important evidence for cold fusion. In this section we discuss the He analysis of Phase I Pd cathodes.

The presence of He in our metal electrodes was detected using mass spectrometric techniques. Samples (10–30 mg) were cut from the Pd electrodes and the apparatus described in Refs. 31 and 32 was used to melt the Pd and collect all escaping gases. The gas sample was then cryogenically separated and the remaining He was analyzed by mass spectrometry. The resulting $^3$He and $^4$He mass peaks were compared with standards for calibration.

A He assay of one of the Phase I samples was obtained,[33] with the result that no enhancement of $^3$He or $^4$He above background levels was detected. This analysis was performed on samples taken from a Pd cathode that had undergone 21 days of electrolysis in 0.1 M LiOD/$D_2O$ electrolyte solution. The results (Table V) indicate that no He above the background level was generated in the Pd cathode.

The He assay provides an upper limit on the average fusion power produced from Eq. (C) (Table I). The He assay of the Pd electrode provides a typical sensitivity of $n_{He} = 4 \times 10^{11}$ atoms/cm$^3$. The upper limit on fusion energy production is obtained by multiplying the sensitivity by the heat of reaction, $Q_{He}$. For the $^4$He branch, $Q_{He}$ = 23.88 MeV/reaction or $3.8 \times 10^{-12}$ J/reaction or 267 Gcal/mol of reaction product. To obtain the average detectable fusion power, the volumetric heat of reaction is divided by the duration of the experiment, $\Delta t$ (Eq. 5).

$$P_{D+D\rightarrow{}^4He} = \frac{n_{He}Q_{He}}{\Delta t} \quad (5)$$

Using the detection sensitivity, heat of reaction, and taking a typical time interval for the electrolysis run to be $\Delta t$ = 250 h, the average detectable fusion power by the He assay method is $P_{D+D\rightarrow{}^4He} < 2$ μW/cm$^3$. A similar analysis for the power from the $^3$He fusion branch (Eq. A, Table I) yields $P_{D+D\rightarrow{}^3He} < 3$ μW/cm$^3$. The He assay technique is approximately $10^3$ times more sensitive than calorimetric measurements that can typically detect heat variations in the 10-mW range. However, for the analyses discussed in this section, only the $^3$He fusion branch will result in solution heating, since the energy associated with the γ-ray of the $^4$He fusion branch will be carried out of the cell.

**Table V.** Results of the He Analysis of Phase I Pd Cathodes[a]

| Sample description | Mass (mg) | $^3$He (atoms/sample) | $^4$He |
|---|---|---|---|
| Before electrolysis | | | |
| Pd cathode 1 | 13.60 | $<1\times10^8$ | $2\times10^8$ |
| Pd cathode 2 | 18.52 | $<1\times10^8$ | $1\times10^8$ |
| After 21 days of electrolysis in $D_2O$ electrolyte[b] | | | |
| Pd cathode 3 | 12.29 | $<1\times10^8$ | $1\times10^8$ |
| Pd cathode 4 | 12.64 | $<1\times10^8$ | $4\times10^8$ |

[a] See Ref. 33.
[b] See Table III.

## 9. SURFACE ANALYSIS OF PD CATHODES

The Pd cathodes were observed to undergo physical changes in Phase I and II experiments. For example, the electrodes expanded, fissures developed, and the color of the surface varied. To understand the nature of these compositional changes an elemental surface analysis (X-ray photoelectron spectroscopy, XPS) was undertaken.

Cathode samples from the Phase II $D_2O$ and $H_2O$ cells, and an unused Pd sample were examined by XPS over the range of binding energies 0–1000 eV.[6] After each analysis, a portion of the surface was removed by $Ar^+$ sputtering to establish a depth profile of contaminants in the surface region. The spectrum shown for a used Pd cathode (Fig. 11a) was recorded after 15 s of $Ar^+$ sputtering. Peaks corresponding to C, O, F, Si, As, Na, Zn, Mg, and Pt are present, but the peak expected for Pd peak is absent. This result indicates that the important catalytic properties associated with a clean Pd surface are obscured in a used cathode since the escape depth of a photoelectron is about 50 Å.[35] After 12 min of $Ar^+$ sputtering peaks arising from Pd emerged, and after 45 min the surface spectrum appeared essentially identical to the spectrum of a fresh Pd sample (Fig. 11b). Surface-bound Li originating in the electrolyte might be expected to be present, but does not appear presumably because XPS is not very sensitive to this element.

The source of surface impurities from electrolytes was not thoroughly investigated, however, we speculate that they originated in the cell materials. For example, Si, As, and Na are present in the Pyrex,[36] and these elements can be leached from the glass in aqueous base.[37] The presence of Pt on the Pd cathode suggests dissolution of Pt at the anode followed by deposition on the cathode.[38] It is likely that C and F originate in the internal Teflon supports. Whatever their source, changes in surface composition of the Pd cathode shown by the spectra in Fig. 11 will exert time-dependent changes in

[6] A Surface Science SSX-100 spectrometer was used to obtain the XPS Spectra.[34]

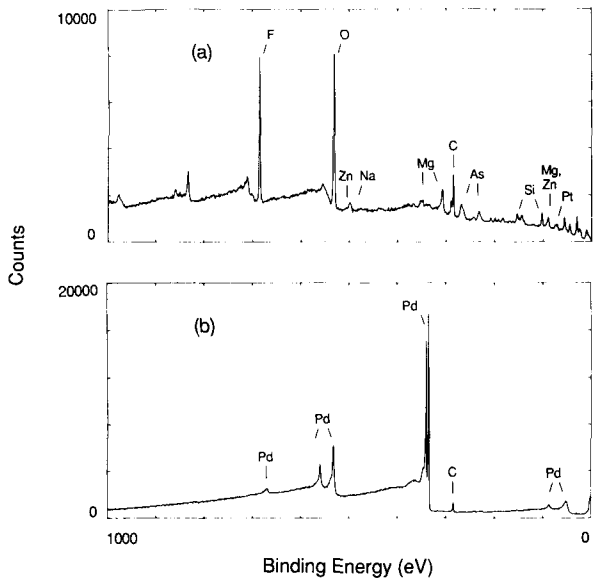


**Fig. 11.** (a) XPS spectrum of the Pd cathode from the Phase II $D_2O$ cell after ~200 h of electrolysis. The surface of the sample was $Ar^+$ sputtered for 15 s before analysis. (b) XPS spectrum of a fresh Pd sample.

parameters critical to calorimetry and the composition of $PdD_n$. For example, changes in surface structure will affect the cell voltage, $V_c$, and therefore the level of power, $P_c$, dissipated in the cell. In addition, it is known that certain adsorbates can change the maximum ratio of D/Pd in electrochemically-charged Pd cathodes.[39]

## 10. CRITIQUE OF THE γ-RAY SPECTROSCOPY

Two sets of γ-ray spectra have been published by FPH as supporting evidence for solid state fusion of deuterons in their experiment.[1,6] In the first spectrum, presented in their original paper and errata,[1] they showed a signal peak centered at 2.22 MeV (Fig. 12a). They contend that this signal line originated from neutron-capture-on-hydrogen (Eq. 1), and therefore was proof of neutron generation in their electrolysis cells. We have found several fundamental inconsistencies with this spectrum. First, the linewidth of the signal line corresponds to a NaI detector resolution of about 2.5% at 2.2 MeV. But based on classical works on NaI scintillation detectors, on our own measurement of γ-rays from neutron-capture in water using 3 in × 3 in NaI detectors, and on their own detector calibration with 1.33 and 1.46 MeV γ lines, their detector resolution at 2.2 MeV should

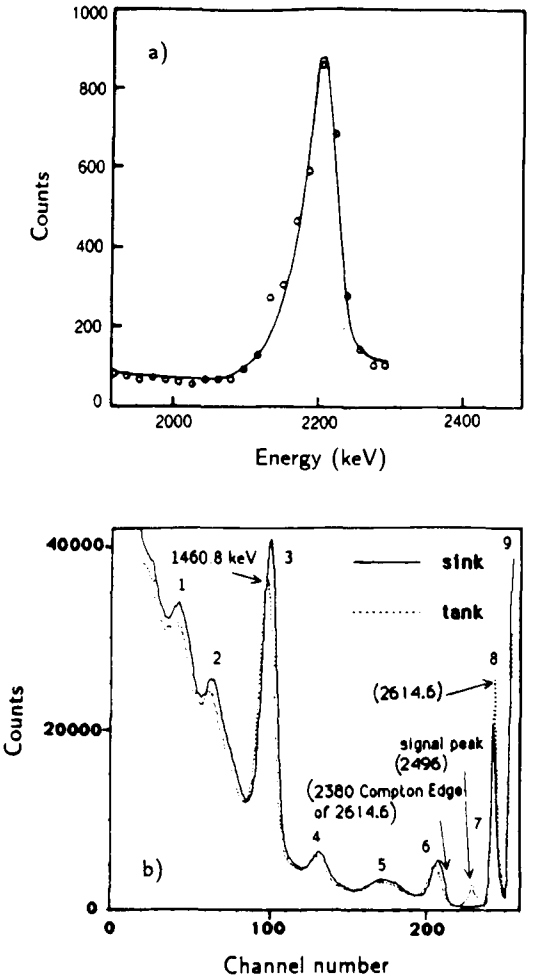


**Fig. 12.** γ signals presented by FPH[1] as supporting evidence of nuclear fusion in electrochemical cells. (a) A reproduction of the purported 2.22 MeV neutron-capture-on-hydrogen γ-ray line.[1] As we pointed out previously,[4] the resolution of their NaI spectrometer would be about 2.5% based on this linewidth. With such resolution, one would expect to see a clearly-defined Compton edge at 1.99 MeV. No edge is evident. Also, a resolution of 2.5% is inconsistent with their spectral resolution (Table 1b in Ref. 4). Because of these inconsistencies, we argue that this signal is an instrumental artefact. (b) A reproduction of the FPH spectrum which contains a 2.496 MeV signal line (peak 7).[6] We argue that the signal line is an instrumental artifact because its lineshape is unphysical.[4] Also, we believe the $^{208}Tl$ (2.61 MeV) line is peak 6 instead of peak 8, as has been identified by FPH. Therefore, the purported signal line is at about 2.8 MeV instead of 2.496 MeV. Furthermore, there is no significant difference between the sink (background) and the tank (cell) spectra at 2.2 MeV, near peak 5. This sets an upper limit on the neutron production rate of 400 n/s from the heat-producing cell. This limit is a factor of 100 smaller than the neutron rate FPH claim to have actually observed.[1]

be 4–5%. Second, no Compton edge is present in their spectrum (Fig. 12a), and it should be distinctly promi-

nent at 1.99 MeV, as shown in Fig. 8a. Third, there are several natural background $\gamma$ lines located near 2.2 MeV. Consequently, the background rate near $E = 2.2$ MeV should be of about the same magnitude as their signal line. The unusually low $\gamma$-ray background shown in their spectrum suggests that their signal line cannot be located at 2.2 MeV. Based on these arguments, we concluded that the FPH signal line is an instrumental artifact unrelated to a $\gamma$ reaction, and that its energy location is unlikely to be 2.2 MeV.[4a]

In response to the above criticism, FPH published a second spectrum (Fig. 12b), which is a full $\gamma$-spectrum claimed to be measured over a cell generating excess heat at a rate of 1.7–1.8 W.[6] In the new spectrum, they identified a signal line at an energy of 2.496 MeV (peak 7, Fig. 12b) rather than at 2.22 MeV. They are not able to identify the physical processes which generates this 2.496-MeV $\gamma$-ray, but they contend that the signal line is still evidence of some unspecified nuclear reaction occurring in their cell. We have pointed out[4] that this new signal line has a shape which is unphysical, and we concluded that it is not a true $\gamma$ line. Furthermore, based on our identification of background lines in their spectrum, we determined that they have misidentified the $^{208}$Tl (2.61 MeV) line, and therefore their energy calibration is incorrect.[4] With the correct energy calibration, their signal peak actually resides at about 2.8 MeV rather than 2.496 MeV. We believe that the high energy peaks (peaks 7–9, Fig. 12b) are caused by defects in the upper channels of their spectrum analyzer. Nevertheless, one crucial observation can be made by comparing the FPH spectra measured over a heat-producing cell and that measured over a sink 5-m away: no observable change exists in the $\gamma$ rate at 2.22 MeV (in the vicinity of peak 5, Fig. 12b). Quantitatively, based on our controlled neutron experiment in water and the FPH $\gamma$ data in the energy range near 2.22 MeV, we can set an upper limit on the neutron production rate of about $4 \times 10^2$ n/s from their cell.[4] This bound is a factor of 100 smaller than the rate FPH claim to have actually observed with their neutron detector.[10] Therefore, we conclude that FPH did not observe neutrons or $\gamma$-rays from their electrochemical cells.

## 11. COMMENTS ON CALORIMETRY

### 11.1. Refinements

There are a number of error sources present in the calorimetry we have described. Some of these are inherent to long-term electrochemical calorimetry,[40] but others can be minimized through careful choice of the calorimeter used and electrolysis conditions. Since the design of our calorimeter was intended to resemble that of FPH, it is likely that many of the difficulties we encountered could also have been present in their experiments. In this section, we will discuss several important aspects of high resolution, long-term electrochemical calorimetry.

In open cell calorimetry, one significant error arises from energy loss due to unintentional recombination of the electrolysis gases, $D_2$ and $O_2$ (Eq. 6).

$$2D_2 + O_2 \rightarrow 2D_2O \qquad (6)$$

Catalytic recombination will take place at Pd or Pt surfaces in either the gas or the liquid phase. As pointed out in Section 11.2, the magnitude of the excess power reported by FPH,[1] and others[7,8] is usually lower than or comparable to the heat-accompanying chemistry released according to Eq. (6). Other important deficiencies of vented cells include energy losses due to evaporation, fluctuations of electrolyte levels, and atmospheric contamination of electrolyte solutions.

Some of the problems associated with open-cell calorimetry can be adequately addressed by intentional recombination of electrolysis gases in a closed-cell configuration. In closed cells, all heat released according to Eq. (6) can be accounted for since no reaction products are permitted to escape the calorimeter. Furthermore, difficulties associated with solution losses to evaporation and electrolysis are not present in closed cells. These losses will affect the thermal mass of the calorimeter and the cell resistance. For example, the thermal drift detected in our calorimeter (Fig. 6) was caused by time-dependent changes in thermal power loss, $P_{th}$. The cell resistance, which is determined by the electrode geometry and the concentration of electrolyte will also be affected by solution loss, since the time-dependent increase in electrolyte concentration will serve to lower the cell resistance, thereby reducing the total cell power, $P_c$. In addition, if the electrolyte level falls so as to reduce the active surface area of either electrode, the current density, and therefore $P_c$, will increase.[41] Evaporative losses will affect power measurements in much the same manner.

The cell materials are another serious source of error in electrochemical calorimetry. As discussed in Section 9, glass is sparingly soluble in alkaline solutions,[37] Pt can transfer from the anode to the cathode,[38] and low molecular weight $(CF_2)_x$ can leach out of Teflon.

There are several other problems which are likely to have adverse effects on electrochemical calorimetry.

For example, gas vented from our cells frequently ceased to flow for extended time periods. This effect was caused by formation of large gas bubbles which became trapped under the upper and lower Teflon supports (Fig. 2a). The effect of bubble formation is similar to that of solvent loss by evaporation or electrolysis. Phase changes within the Pd lattice ($\alpha_{Pd} \rightarrow \beta_{Pd}$), time-dependent changes in electrode surface roughness, temperature gradients caused by ineffective stirring, inadequate methods of power calibration, and redistribution of electrolyte in the cell caused by condensation and droplet formation all represent deficiencies in calorimetry.

Considering the higher resolution afforded by many of the fusion product assay techniques compared to heat-based calorimetry, we feel that demonstration of cold fusion will be better served by focusing detection efforts on fusion products rather than power measurements.

### 11.2. Critique of the Calorimetric Results

An important aspect of the FPH experiment stems from the claim that thermal power was generated with a magnitude of several W/cm$^3$, and that this level of power is orders of magnitude larger than can be accounted for by chemical processes. We have analyzed the calorimetry data presented in Tables I and II in Ref. 1, and find that the above claims are incorrect and not supported by the data. The excess heat reported, more correctly the excess power, $P_x$, is less than or approximately equal to the energy associated with the chemistry of Eq. (6). Table VI contains data from Ref. 1 concerning the cathode dimensions, current density, total cell current, excess power, $P_{ex}$, recombination power, $P_{rec}$ (1.53 V $\times$ $I_c$), and the ratio of the excess power to recombination power, $P_{ex}/P_{rec}$. Table VI shows that in seven out of nine cases $P_{ex} < P_{rec}$. In one of the remaining cases, the value of $P_{ex}$ was scaled by an unspecified method from a cathode length of 1.25 cm to a length of 10 cm. In the other case, the difference between $P_{ex}$ and $P_{rec}$ may not be significant considering the numerous error sources inherent to open-cell calorimetry. On the basis of the analysis presented here, we believe that the calorimetry data reported by FPH do not support the claim that "It is inconceivable that this [power] could be due to anything but nuclear processes."[1]

## 12. SUMMARY

We have designed and implemented experiments intended to duplicate those reported by FPH.[1] Our analyses are broad-based and include measurements of neutron and $\gamma$ radiation, power, and fusion products. In all cases, the minimum detection limits in our experiments are better than, or equivalent to those reported by FPH. Importantly, the level of fusion products present is by far a more sensitive indicator of nuclear fusion reactions than are the relatively insensitive heat-based measurements which form the foundation of the claim of cold nuclear fusion put forth by FPH.[1] At our level of sensitivity, which in some cases corresponds to a level $10^7$ times better than the rate of excess heating claimed by FPH, we have not detected any evidence for nuclear fusion processes or any excess power generation in electrochemical cells containing $D_2O$ and Pd cathodes. Furthermore, based on our critique[4] of the FPH $\gamma$ spectra, we conclude that FPH, contrary to their claims,[1,6] did not detect neutrons or $\gamma$-rays from their "excess heat-producing" cells.

**Table VI.** Analysis of FPH Calorimetry Data

| Cathode dimension (cm) | Current density (mA/cm$^2$) | Cell current (mA) | Excess power, $P_{ex}$ (W) | Recombination power, $P_{rec}$ (W) | $P_{ex}/P_{rec}$ |
|---|---|---|---|---|---|
| 0.1 × 10 | 8 | 25 | 0.0075 | 0.0385 | 0.19 |
| 0.1 × 10 | 64 | 201 | 0.079 | 0.31 | 0.25 |
| 0.1 × 10[a] | 512 | 1610 | 0.65 | 2.48 | 0.26 |
| 0.2 × 10 | 8 | 50 | 0.036 | 0.077 | 0.46 |
| 0.2 × 10 | 64 | 402 | 0.493 | 0.619 | 0.79 |
| 0.2 × 10[a] | 512 | 3220 | 3.02 | 4.96 | 0.61 |
| 0.4 × 10 | 8 | 101 | 0.15 | 0.155 | 0.97 |
| 0.4 × 10 | 64 | 804 | 1.75 | 1.24 | 1.41 |
| 0.4 × 10[a] | 512 | 6430 | 26.8 | 9.90 | 2.71 |

[a] Data scaled from 1.25-cm length cathodes to 10-cm length.[1]

## ACKNOWLEDGMENTS

This work was supported in part by the United States Department of Energy contract number DE-AC02-78ET51013. We would like to thank Robert H. Childs, Edward W. Fitzgerald, Mitchell Galanek, David A. Gwinn, Christian Kurz, Frederick F. McWilliams, John C. Nickerson, James A. Simms, Edward J. Takach, and Cornelis L. H. Thieme for technical assistance (MIT). In addition, we acknowledge Brian Oliver of Rocketdyne for obtaining the He analysis discussed in Section 8.

## REFERENCES

1. M. Fleischmann, S. Pons, and M. Hawkins (1989). *J. Electroanal. Chem.*, **261**, 301; **263**, 187.
2. S. E. Jones, E. P. Palmer, J. B. Czirr, D. L. Decker, G. L. Jensen, J. M. Thorne, S. F. Taylor, and J. Rafelski (1989). *Nature,* **338**, 737.
3. A. DeNinno, A Frattolillo, G. Lollobattista, L. Martinia, M. Martone, L. Mori, S. Fodda, and F. Scaramuzzi (1989). *Europhys. Lett.*, **9**, 221.
4. R. D. Petrasso, X. Chen, K. W. Wenzel, R. R. Parker, C. K. Li, and C. Fiore (1989). *Nature,* **339**, 183;667.
5. M. Fleischmann (1989). As we have repeatedly pointed out, we are well aware of the deficiencies of these [γ-ray] spectra. 175th Meeting of the Electrochemical Society, Los Angeles, California, May 1989; J. Maddox (1989). *Nature,* **340**, 15.
6. M. Fleischmann, S. Pons, M. Hawkins, and R. J. Hoffman (1989). *Nature,* **339**, 667.
7. A. J. Appleby, S. Srinivasan, Y. J. Kim, O. J. Murphy, and C. R. Martin (1989). Presented at the Workshop on Cold Fusion Phenomena, Santa Fe, New Mexico, May 23–25.
8. A. Belzner, U. Bischler, S. Crouch-Baker, T. M. Gur, F. Lucier, M. Schreiber, and R. A. Huggins (1989). Presented at the Workshop on Cold Fusion Phenomena, Santa Fe, New Mexico, May 23–25.
9. K. L. Wolf, N. Packham, J. Shoemaker, F. Cheng, and D. Lawson (1989). Presented at the Workshop on Cold Fusion Phenomena, Santa Fe, New Mexico, May 23–25.
10. *Meeting abstracts and abstracts selected for poster sessions.* (1989). Workshop on Cold Fusion Phenomena, Santa Fe, New Mexico, May 23–25.
11. G. Horanyi (1989). *Electrochim. Acta,* **34**, 889.
12. S. E. Koonin and M. Nauenberg (1989). *Nature,* **339**, 690.
13. A. J. Leggett and G. Baym (1989). *Nature,* **340**, 45.
14. 179th American Chemical Society National Meeting, Dallas, Texas, April 1989.
15. 175th Meeting of the Electrochemical Society, Los Angeles, California, May 1989.
16. F. K. McGowan *et al.* (1969). *Nuclear Data Tables,* **A6**, 353; **A8**, 199 (1970).
17. S. E. Jones (1986). *Nature,* **321**, 127.
18. T. Graham (1966). *Phil. Trans. Roy. Soc. (London),* **156**, 415.
19. F. A. Lewis (1967). *The Palladium Hydrogen System* (Academic Press, London,
20. J. E. Worsham, Jr., M. K. Wilkinson, and C. G. Shull (1957). *J. Phys. Chem. Soln.*, **3**, 303.
21. L. L. Lohr, *J. Phys. Chem.* (1989). **93**, 4697.
22. Z. Sun and D. Tománek (1989). *Phys. Rev. Lett.*, **63**, 59.
23. D. P. Smith (1948). *Hydrogen in Metals* (The University of Chicago Press, Chicago).
24. E. Wicke, H. Brodowsky, and H. Züchner (1978). In *Hydrogen in Metals II, Topics in Applied Physics* (Vol. 29) G. Alefeld and J. Völkl, eds. (Springer-Verlag, Berlin), Vol. 29.
25. G. Sicking (1972). *Ber. Bunsenges. Phys. Chem.*, **76**, 790.
26. W. F. Reilly (1959). Construction and calibration of a standard pile, M.S. Thesis, M.I.T., Cambridge, MA, (b) M. E. Anderson, *Nucl Appl.*, **4**, 142 (1968).
27. J. P. Hoare (1985). In *Standard Potentials in Aqueous Solutions* (Chap. 4), A. J. Bard, R. Parsons, and J. Jordan, eds. (Dekker, New York).
28. C. Walling and J. Simons (1989). *J. Phys. Chem.*, **93**, 4693.
29. G. J. Thomas and J. M. Mintz (1983). *J. Nucl. Mat.*, **116**, 336; T. Schober (1986). In *Hydrogen in Disordered and Amorphous Solids,* G. Bambakidis and R. C. Bowman, Jr., eds. (Plenum, New York), pp. 377–396.
30. *CRC Handbook of Chemistry and Physics,* edited by R. C. Weast, (CRC Press, Boca Raton, FL, 1985), p. F156.
31. M. D. Kurz, W. J. Jenkins, and S. R. Hart, *Nature,* **297**, 6, 43 (1982).
32. M. D. Kurz, W. J. Jenkins, J. C. Schilling, and S. R. Hart, *Earth Planet. Sci. Lett.*, **58**, 1 (1982).
33. Brian Oliver, Rocketdyne Division, Rockwell International, Canoga Park, CA.
34. P. Laibinis, J. Hickman, M. S. Wrighton, and G. Whitesides (1989). *Science* (in press).
35. M. P. Seah and W. A. Dench (1979). *Surface and Interface Analysis,* **1**, 2.
36. D. C. Boyd and D. A. Thompson (1980). *Kirk–Othmer Encyclopedia of Chemical Technology* (Wiley, New York), pp. 807–880.
37. *The Corning Laboratory Catalogue* (1988). (Corning Science Products, Corning, New York), p. T7.
38. P. Malachesky, R. Jasinski, and B. Burrow (1967). *J. Electrochem. Soc.*, **114**, 1104; S. Ya. Vasina, O. A. Petrii, and V. A. Safanov (1981). *Elektrokhimiya,* **17**, 270.
39. T. Maoka and N. Enyo (1981). *Electrochim. Acta,* **26**, 607.
40. J. M. Sherfey and A. Brenner (1958). *J. Electrochem. Soc.,* **105**, 665.
41. A. J. Bard and L. R. Faulkner (1980). *Electrochemical Methods* (Chap. 3) (Wiley, New York).